

SPHERICAL WAVELET DESCRIPTORS FOR CONTENT BASED 3D MODEL RETRIEVAL

Hamid Laga Hiroki Takahashi Masayuki Nakajima

Graduate School of Information Science and Engineering,
Tokyo Institute of Technology, Japan
email: {hamid,rocky,nakajima}@img.cs.titech.ac.jp

ABSTRACT

The description of 3D shapes with features that possess descriptive power is one of the most challenging issues in content based 3D model retrieval. In this paper we propose the usage of spherical wavelet transform as a tool for the analysis of 3D shapes represented by functions on the unit sphere. We introduce three new shape descriptors extracted from the spherical wavelet coefficients, namely: (1) a subset of the spherical wavelet coefficients, (2) the L_1 and, (3) the L_2 energies of the spherical wavelet sub-bands. The advantage of this tool is three fold: First, it filters out small shape details which hamper the retrieval performance. Second, it takes into account feature localization and local orientations. Third, it allows shape matching at different resolutions. Spherical wavelet descriptors are natural extension of 3D Zernike moments and spherical harmonics. We evaluate, on the Princeton Shape Benchmark, the proposed descriptors regarding computational aspects and shape retrieval performance.

1. INTRODUCTION

The 21st century is the era of digital media and a substantial progress has been achieved in acquisition, storage and transmission of different types of information. While text, images, sound and video have been the predominant form of digital media, 3D models emerge as a new form. They have applications in many fields including CAD, medicine, physical simulation, e-commerce and education. Consequently, a significant research effort is spent to developing effective techniques for 3D model retrieval.

A challenging issue in content based 3D model retrieval is the description of a model with a suitable numerical representation called *shape descriptor*. In general a shape descriptor should be discriminative, compact, easy to compute, and invariant under a group of transformations. While invariance to global transformations, such as translation, rotation, scale [5, 12, 22], and invariance under certain deformations [7, 19], have been extensively studied, existing shape descriptors have difficulties to handle local variation in scale and orientations. On the other hand, small details in the shape hamper the performance of many descriptors. Similarity measures need to be computed at optimal translation, rotation and scale. Moreover, they should capture only the key shape features.

Most of three-dimensional shape retrieval techniques proposed in the literature aim to extract from the 3D model meaningful descriptors based on the geometric and topological characteristics of the object. Survey papers to the related literature have been provided by Tangelder et. al [20] and Iyer et. al [9]. They fall into three broad categories: feature-based including global and local features, graph-based and view-based similarity.

View-based techniques compare 3D objects by comparing their two dimensional projections. The Lightfields [1] are reported to be the most effective descriptor [18]. View-based techniques are suitable for implementing query interfaces using sketches [9, 6].

Graph-based techniques reduce the problem of shape dissimilarity estimating to the problem of comparing graphs. They are suitable for retrieving articulated objects, and the Reeb graph proposed by Hilaga *et al.* [7] is among the most popular. Other techniques include methods based on the distribution of features such as shape distributions [15], and local features such as spin [11]. Shilane et. al. [18] provides a comparison of these techniques and reported that histogram based techniques are the less efficient in term of discriminative power.

Feature-based methods aim to extract a compact descriptor from the 3D object. A common approach is to represent the shape using functions defined on the unit sphere. Funkhouser et al. [6] uses spherical harmonics (SH) to analyze the shape function. They demonstrated later that the spherical harmonics can be used to achieve rotation invariance provided that the shape function is defined on the sphere [12]. Novotni et. al. [13] uses 3D Zernike moments (ZD) as a natural extension of SH. Representing 3D shapes as functions on concentric sphere have been extensively used [12]. Our developed descriptors fall into this category and are a natural extension of SH and ZD.

In this paper we present a new 3D content based retrieval method relying on spherical wavelet transform (SWT). Spherical Wavelets have been introduced by Schröder et. al. [17] and since, they have been used to solve many geometry processing problems including 3D model compression [8]. Similar to first generation wavelets [2, 10], SWT are an effective tool to analyze shape functions defined on the sphere S^2 as they provide a natural partition of the function spectrum into multiscale and oriented sub-bands.

To the best of our knowledge, SWT have not been applied to content based retrieval of 3D models so far. We

make use of these results and propose three new descriptors, namely: spherical wavelet coefficients as feature vector (SWC_d), L1 energy of the spherical wavelet coefficients (SWEL1), and L2 energy of the spherical wavelet coefficients (SWEL2). In particular SWEL1 and SWEL2 are compact, easy to compute and compare and rotation invariant. Spherical wavelet descriptors are a natural extension of spherical harmonics [6] and 3D Zernike moments [13, 14]. They offer better feature localization and takes all the advantages of wavelets over Fourier analysis.

This paper begins by reviewing in Section 2 the general concepts of spherical wavelet transform of functions on the sphere. Section 3 describes in detail how our new shape signatures are extracted. Section 4 presents some experimental results. Finally, we summarize the main findings and issues for future research in Section 5.

2. SPHERICAL WAVELETS FOR SHAPE ANALYSIS

In the context of 3D shape analysis, it is common to represent a 3D model as a function f sampled on the unit sphere:

$$\begin{aligned} f: \mathcal{S}^2 &\rightarrow \mathbb{R}^+ \\ f(u) &= f(\theta, \phi). \end{aligned}$$

where θ and ϕ are respectively, the azimuthal and polar angles. We use spherical Extent function (EXT) which measures the maximal distance from the center of mass to the surface as a function of spherical angle (θ, ϕ) [16].

2.1. Spherical wavelets

Wavelets are basis functions which represent a given signal at multiple levels of detail, called *resolutions*. They are suitable for sparse approximations of functions. In the Euclidean space, wavelets are defined by translating and dilating one function called *mother wavelet*. In \mathcal{S}^2 , however, the metric is no longer Euclidean. Schröder et. al. [17] introduced the second generation wavelets. The idea behind was to build wavelets with all desirable properties adapted to much more general settings than real lines and 2D images.

The general wavelet transform of a function λ is constructed as follows:

$$\begin{aligned} \text{Analysis:} \quad \lambda_{j,k} &= \sum_{l \in K(j)} \tilde{h}_{j,k,l} \lambda_{j+1,l} \\ \gamma_{j,k} &= \sum_{l \in M(j)} \tilde{g}_{j,m,l} \lambda_{j+1,l} \end{aligned}$$

$$\text{Synthesis:} \quad \lambda_{j+1,l} = \sum_{k \in K(j)} h_{j,k,l} \lambda_{j,k} + \sum_{m \in M(j)} g_{j,m,l} \gamma_{j,m}$$

where $\lambda_{j,\bullet}$ and $\gamma_{j,\bullet}$ are respectively the approximation and the wavelet coefficients of the function at resolution j . The analysis process is performed recursively on the function $\lambda = \lambda_{n,\bullet}$ at the finest resolution n , to get $\gamma_{j,\bullet}$ at level j , $j = n - i, \dots, n - 1$. The coarsest approximation $\lambda_{n-i,\bullet}$ is obtained after $i, 0 < i < n$ iterations.

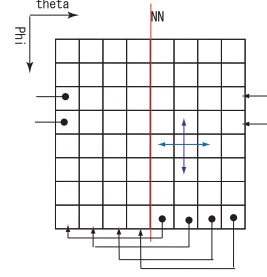


Fig. 1. Spherical wavelet transform: domain setting.

The natural extension of Euclidean translations are rotations on sphere \mathcal{S}^2 . The sets $M(j)$ and $K(j)$ are now index sets on the sphere such that $K(j) \cup M(j) = K(j+1)$, and the line distance is replaced by arc distances. The decomposition filters \tilde{h}, \tilde{g} , and the synthesis filters h, g denote spherical wavelet basis functions.

2.2. Analysis of the spherical shape function

To analyze a 3D model, we first apply spherical wavelet transform (SWT) to the spherical shape function and collect the coefficients to construct discriminative descriptors. The properties and behavior of the shape descriptors are therefore determined by the spherical wavelet basis functions used for transformation.

Similar to 3D Zernike moments [13] and spherical harmonics [12, 22], the desired properties of a descriptor are: (1) Invariance to a group of transformations, (2) Orthonormality of the decomposition, and (3) Completeness of the representation. The orthonormality ensures that the set of features will not contain redundant information. The completeness property implies that we are able to reconstruct approximations of the signal from the decomposition.

The SW basis function should reflect these properties. In our implementation we experimented with Haar wavelets which are orthogonal, have a compact support and one vanishing moments. Other SWT can also be used, and an in depth analysis of their performance is required, which is beyond the scope of this paper.

In practice, the shape function is decomposed into an approximation part and detail parts by applying low pass and high pass filters in horizontal and vertical directions. Here, we mean by horizontal the direction along the azimuthal angle θ , and by vertical the polar direction (angle ϕ). The approximation part is recursively decomposed until the coarsest level is reached. Finally, the approximation and the SW coefficients are collected and will be used to build the shape descriptor. Algorithm 1 summarizes the process. Lets denote by:

- \mathcal{L}_h and \mathcal{L}_v : one dimensional low pass filters in the horizontal and vertical direction respectively.
- \mathcal{H}_h and \mathcal{H}_v : one dimensional high pass filters in the horizontal and vertical direction respectively.

In our implementation we used similar filter in horizontal and vertical directions, i.e: $\mathcal{L}_h = \mathcal{L}_v$ and $\mathcal{H}_h = \mathcal{H}_v$. Issues

to consider are the setting of the neighborhood graph and the distance measure:

- **Neighborhood graph:** As the spherical function is regularly sampled along the azimuthal and polar axis, we use the regular neighborhood graph illustrated in Figure 1. The boundaries however require a careful processing. In our implementation we chose the image-like structure: we use spherical neighborhood graph at the north and south poles, and cylindrical neighborhood at the eastern and western boundaries.
- **Distance measure:** As the metric is not Euclidean, an edge in the geometry image is an arc on the sphere, inherent to the sphere sampling method, the edges have different lengths (longer near the equator and short at the north and south poles).

Algorithm 1: Spherical wavelet transform algorithm

Input: Geometry image I representing the 3D model;
 $size(I) = 2^n \times 2^n$; Number of decomposition levels
 $l, 0 < l < n$;

Output:

Initialization: $I^{(n)} \leftarrow I$;

$i \leftarrow 0$;

repeat

- Apply \mathcal{L}_h in horizontal direction to $I^{(L-i)}$:
 $\mathcal{L}_h(I^{(n-i)}) = I_{low}$;
- Apply \mathcal{H}_h in horizontal direction to $I^{(L-i)}$:
 $\mathcal{H}_h(I^{(n-i)}) = I_{high}$;
- Apply \mathcal{L}_v in vertical direction to I_{low} , we get the approximation $I^{(n-(i+1))}$: $\mathcal{L}_v(I_{low}) = I^{(n-(i+1))}$;
- Apply \mathcal{H}_v in vertical direction to I_{low} , we get the vertical detail $V^{(n-(i+1))}$:

$$\mathcal{H}_v(I_{low}) = V^{(n-(i+1))}$$

- Apply \mathcal{L}_v in vertical direction to I_{high} , we get the horizontal detail $H^{(n-(i+1))}$:

$$\mathcal{L}_v(I_{high}) = H^{(n-(i+1))}.$$

- Apply \mathcal{H}_v in vertical direction to I_{high} , we get the diagonal detail $D^{(n-(i+1))}$:

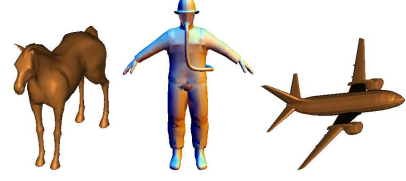
$$\mathcal{H}_v(I_{high}) = D^{(n-(i+1))}.$$

Build the shape descriptor:

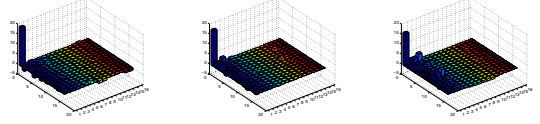
until until $i = l$;

3. SPHERICAL WAVELET-BASED DESCRIPTORS

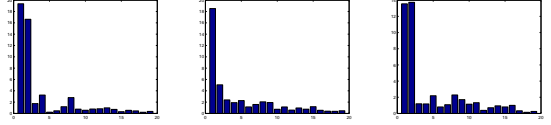
Using spherical wavelet transform, a geometry image I of size $2^n \times 2^n$ is decomposed into $l(0 < l < n)$ levels. At each decomposition level $i, i = 1 \dots l$, we obtain three sub-band coefficients $H^{(n-i)}, V^{(n-i)}$ and $D^{(n-i)}$ of size $2^{n-i} \times 2^{n-i}$. The approximation image A of size $2^{n-l} \times 2^{n-l}$ is obtained at the last decomposition level l . The wavelet coefficients are indicated by $\{x_{i,1}^{dir}, x_{i,2}^{dir}, \dots, x_{i,k_i}^{dir}\}$ where $k_i = 2^{n-i} \times 2^{n-i}$ and $dir \in \{h, v, d, a\}$ which stand for horizontal, vertical, diagonal and approximation, respectively. That is:



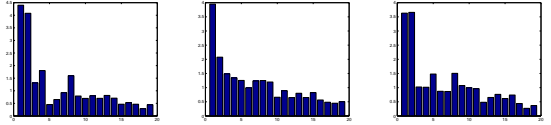
(a) 3D shapes



(b) Spherical wavelet coefficients as descriptor (SWC4).



(c) L_2 energy descriptor (SWEL2).



(d) L_1 energy descriptor

Fig. 2. Example of different models with their spherical wavelet-based descriptors.

- $H^{(n-i)} = \{x_{i,1}^h, x_{i,2}^h, \dots, x_{i,k_i}^h\}$.
- $V^{(n-i)} = \{x_{i,1}^v, x_{i,2}^v, \dots, x_{i,k_i}^v\}$.
- $D^{(n-i)} = \{x_{i,1}^d, x_{i,2}^d, \dots, x_{i,k_i}^d\}$.

For simplicity of notation and when the three directions and the approximation images are treated equally we omit the upscript. Notice that, the wavelet transform generates $2^n \times 2^n$ coefficients independently of the number of decomposition levels.

We propose three methods to compare 3D shapes using their spherical wavelet: (1) Wavelet coefficients as a shape descriptor (SWCd) where the shape signature is built by considering directly the spherical wavelet coefficients, and (2)spherical wavelet energies (SWEL1 and SWEL2). We investigate both the L_1 and L_2 energies. Figure 2 shows three models and their SW descriptors. The following sections detail each method.

3.1. Wavelet coefficients as a shape descriptor

A straightforward approach is to build a shape descriptor using directly the spherical wavelet coefficients. Given the spherical wavelet decomposition of a geometry image I of a 3D object \mathcal{O} , we arrange the coefficients into a 2D lattice $\mathcal{F} = \{\mathcal{F}(i, j)\}$ of size $N = w \times h = 2^n \times 2^n$. The dissimilarity between three dimensional objects \mathcal{O}_1 and \mathcal{O}_2 is given

by the L_2 distance of their descriptors \mathcal{F}_1 and \mathcal{F}_2 :

$$l_2(\mathcal{F}_1, \mathcal{F}_2) = \sqrt{\sum_{i=1}^w \sum_{j=1}^h (\mathcal{F}_1(i, j) - \mathcal{F}_2(i, j))^2} \quad (1)$$

For typical geometry images of size $2^7 \times 2^7$, the dimension of the feature space is $16K$ ($K = 1000$). Therefore, the descriptor is expensive in term of storage requirements and computation time for similarity estimation.

Spherical wavelet decomposition generates a multi-resolution representation of the shape function, where the shape details are encoded in the detail coefficients at highest layers of the pyramid, while the lowest layers approximate the 3D shape. In general, many of wavelet coefficients of the function are either zero or negligible known by *the sparsity* property. On the other hand, not all the coefficients contribute equally to the shape description. This is known by the *saliency* of the features. Moreover, high frequency coefficients affect negatively the discrimination power of the shape descriptor.

Based on these properties, we have tested experimentally on the Princeton Shape Benchmark different lengths of the spherical wavelet based descriptors. For $d = 1 \dots n, n = 7$ we generate shape descriptors of size $2^d \times 2^d$ by truncating the $n - d$ detail images. We call the obtained shape descriptor SWC_d , where $d = 1, \dots, n$, and measure their performance for nearest neighbor, first tier, second tier, E-measure and Discount Cumulative Gain. We found that the performance of the descriptor increases from $d = 1$ to $d = 4$ and then starts decreasing suggesting that fine details contribute negatively to the shape description, while for $d < 4$ important details are lost. In our experiments we use SWC_4 .

This approach performs as a filtering of the 3D shape by removing outliers. A major difference with spherical harmonics is that SWT preserves the localization and orientation of local features. However, a feature space of dimension 256 is still computationally expensive.

Pose normalization

Comparing directly wavelet coefficients requires efficient alignment of the 3D model prior to wavelet transform. A popular method for finding the reference coordinate frame is pose normalization using Principal Component Analysis (PCA) [5], and continuous PCA [23].

We perform the pose normalization in three steps; First we translate the shape's center of mass to the origin $(0, 0, 0)$. Then we align the shape to its principal axis using continuous PCA [23]. We use the maximum area technique to resolve for the the positive and negative directions of the principal axis. Finally we scale the shape such that the average distance between the center of mass to any point in the surface is equal to $1/2$.

3.2. Spherical Wavelet Energy Signatures

Using the observation that rotating a spherical function does not change its energy, we propose to use it to build a shape descriptor. Its benefits are two fold: first it guarantees

rotation invariance without prior pose normalization. Second, it is used to reduce the storage and the computation time required for comparison.

The wavelet energy signatures have been proven to be very powerful for texture characterization [21]. Commonly the L_2 and L_1 norms are used as measures [3, 4]:

$$\mathcal{F}_i^{(2)} = \left(\frac{1}{k_i} \sum_{j=1}^{k_i} x_{i,j}^2 \right)^{\frac{1}{2}} \quad (2)$$

$$\mathcal{F}_i^{(1)} = \frac{1}{k_i} \sum_{j=1}^{k_i} \|x_{i,j}\| \quad (3)$$

A Spherical Wavelet Energy signature is computed for each detail geometry image yielding into a one-dimensional shape descriptor $\mathcal{F} = \{\mathcal{F}_i^{dir}\}, i = 1 \dots l$, and $dir \in \{h, v, d\}$. For geometry images of size $2^7 \times 2^7$, i.e, $n = 7$ and if $l = 6$ decomposition steps are performed, the size of the feature vector is then $N = 3 \times l = 3 \times 6 + 1 = 19$. The components are packed into a one dimensional feature vector $\mathcal{F} = \{\mathcal{F}_i, i = 1 \dots N\}$. We refer to L_1 energy and L_2 energy-based descriptors by **SWEL1** and **SWEL2** respectively.

The main advantage of this descriptor is its compactness, and it is rotation invariant. However, information such as feature localization are lost in the energy spectrum.

3.3. Similarity metrics

Since 3D shapes are now represented as N-dimensional vectors with real-valued components, a natural way to compute distances vectors in the feature space is to use a vector norm, called also L_p norm, (Equation ??).

Let $\mathcal{F} = (f_1, \dots, f_N)$, $\mathcal{F}' = (f'_1, \dots, f'_N) \in \mathbb{R}^N$ be two feature vectors. The dissimilarity between the 3D shapes is given by the L_p distance between \mathcal{F} and \mathcal{F}' :

$$d_p(\mathcal{F}, \mathcal{F}') = \left(\sum_{i=1}^N |f_i - f'_i|^p \right)^{\frac{1}{p}}, p \in \{1, 2 \dots\} \quad (4)$$

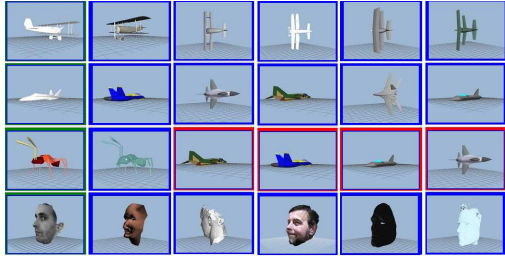
In our implementation we experimented with the L_2 distance.

Note that the introduced spherical wavelet analysis framework supports retrieval at different acuity levels. In some situations, only the main structures of the shapes are required for comparison, while in others, fine details are essential. In the former case, shape matching can be performed by considering only the wavelet coefficients at large scales, while in the later, coefficients at small scales are used. Hence the flexibility of the developed method benefits different retrieval requirements.

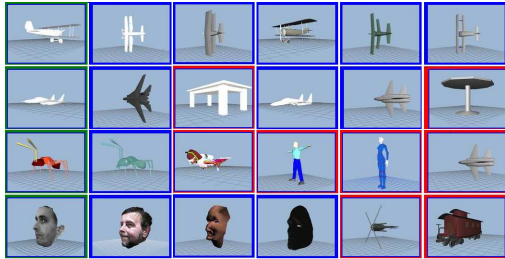
Finally, Table 1 summarizes the length of the proposed descriptors. Note that SWEL1 and SWEL2 are more efficient in term of storage requirement and computation. They are also rotation invariant. Their discrimination efficiency will be discussed in Section 4.

4. EXPERIMENTAL RESULTS

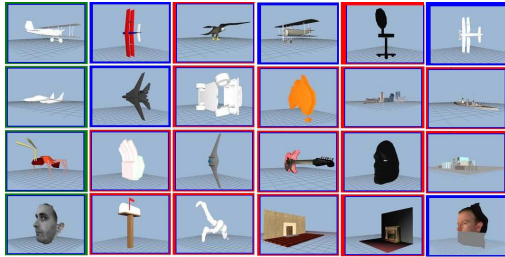
We have implemented the algorithms described in this paper and evaluated their performance on the Princeton Shape



(a) Retrieval results using spherical wavelet coefficients as shape descriptor.



(b) Retrieval results using spherical wavelet L1-energy (SWEL1).



(c) Retrieval results using spherical wavelet L2-energy (SWEL2).

Fig. 3. Retrieval results using spherical wavelet-based shape descriptors. The query model is plotted in green, the correctly retrieved shape are indicated in blue, and the others in red.

Benchmark (PSB)[18]. We represent each model using Spherical Extent Function (EXT) of resolution $128 \times 128 = 2^7 \times 2^7$, i.e: $n = 7$ along the azimuthal and polar angles. A feature index table is built for each of our descriptors. We use six decomposition levels ($l = 6$). SWC_d requires pose normalization while SWEL1 and SWEL2 are rotation invariant.

4.1. Retrieval results

First we executed series of shape matching experiments on base test classification of the PSB. We select randomly a 3D polygon soup model, and then compare it to the objects in the database. We show in Figure 3 the results of several queries for each of our three descriptors SWC_d , SWEL1 and SWEL2. Five most similar objects are displayed. A retrieved model is considered relevant if it belongs to the same class as the query model. The relevant retrieved models are plotted in blue, others in red, and the query model in green.

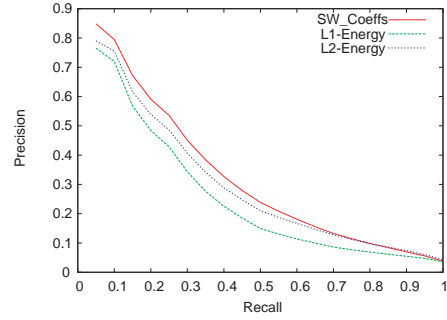


Fig. 4. Precision-recall curves for SW-based descriptors.

Table 1. Performance of SW descriptors on the PSB base test classification, values are in (%).

	length	NN	1 st tier	2 nd tier	E-measure	DCG
SWC ₄	256	55.4	35.5	43.4	23.8	64.7
SWEL1	19	43.7	29.2	40.1	22.3	63.0
SWEL2	19	40.8	26.0	34.9	17.2	59.2

4.2. Performance evaluation

Figure 4 shows the precision-recall curves on the base classifications of the PSB for the three shape signatures. We found that the SWC₄ outperforms SWEL1 and SWEL2 in term of average precision-recall metric.

We evaluated the performance of our descriptors using the nearest neighbor, first and second-tier, E-measure and Discount Cumulative Gain measures [18]. The results are summarized in Table 1. This comes to confirm the visual evaluation, that is, spherical wavelet coefficients perform better, while the L1 and L2 energy comes in the second and third rank respectively. Note that the SWC₄ requires more storage and comparison time.

Similarly we compare our descriptors to the: (1) **Lightfields descriptors (LFD)** [1] considered as the best descriptor, (2) **Spherical harmonic descriptors (EXT)** [16, 12]: extracted from the Spherical Extent function, and (3) **Osada’s D2 Shape distribution** [15]. Shilane et. al. [18] summarized their performance and we use their results to compare with our descriptors.

Table 2 shows the results according to the quantitative measures computed on these three descriptors (the results are the one reported in the original paper [18]).

These results indicate that, spherical wavelet descriptors perform better than shape distributions and spherical harmonic descriptors on precision/recall measures. An interesting observation is that the lightfield descriptor, which is considered a very good signature [18], performs slightly better than spherical wavelet descriptors for the k -nearest neighbors related measures (nearest neighbor, first and second tier), while the spherical wavelet descriptors perform slightly better than the lightfields descriptor for the precision/recall measures (DCG), which are considered more indicative.

Spherical wavelet based descriptors have several benefits over lightfields, shape distributions and spherical harmonic

Table 2. Performance of the LFD, EXT, and D2 on the PSB base classification [18], values are in (%)

	length	NN	1 st – tier	2 nd – tier	E-measure	DCG
LFD	4,500	65.7	38.0	48.7	28.0	64.3
EXT	16	54.9	28.6	37.9	21.9	56.2
D2	64	31.1	15.8	23.5	13.9	43.4

descriptors in terms of storage and computational costs. Table 1 and 2 summarize the length of each shape descriptor.

A comparison with the performance of the EXT descriptor shows clearly that spherical wavelet transform performs better than spherical harmonic transform. Particularly the SWEL1 has several benefits: (1) compactness, (2) rotation invariant without pose normalization, and (3) easy to compute compared to spherical harmonic transform.

5. CONCLUSIONS AND FUTURE WORK

We proposed in this paper, a spherical wavelet-based framework for the analysis of 3D shapes represented by functions on the sphere. We developed and tested using the Spherical Extent Function three new shape descriptors. Our results on the Princeton Shape Benchmark show that the new framework outperforms in term of precision-recall measures the spherical harmonic based descriptor.

Our best results have been achieved using SWC₄ after efficient pose normalization, while the SWEL1 and SWEL2 energy performance compare to the power spectrum. The SWEL1 and SWEL2 are equivalent to the power spectrum of the spherical harmonic analysis. They have many desirable properties. First they are compact and faster to compute, and invariant under similarity transformations. We argue this improvement in the performance by the fact that spherical wavelet transform filters small details that affect negatively the performance, while it takes into account the spatial localization of the salient features.

This work suggests a number of challenges that we would like to consider in the future. First the proposed descriptors have been tested using only the Spherical Extent function. We will experiment with other shape spherical functions. Second, we plan to test the proposed descriptors on other 3D model databases. Another issue is to experiment with different SW basis and compare their performance on different classes of shapes. Finally, none of the developed descriptors perform equally in all situations and on all classes of shapes. A challenging issue is to investigate on how to combine and select features in order to achieve best performance.

6. REFERENCES

- [1] D.-Y. Chen, X.-P. Tian, Y.-T. Shen, and M. Ouhyoung. On visual similarity based 3d model retrieval. *Computer Graphics Forum*, 22(3):223–232, 2003.
- [2] I. Daubechies. *Ten lectures on wavelets*. Society for Industrial and Applied Mathematics, Philadelphia, PA, USA, 1992.
- [3] M. N. Do and M. Vetterli. Texture similarity measurement using kullback-leibler distance on wavelet subbands. In *ICIP*, 2000.
- [4] M. N. Do and M. Vetterli. Wavelet-based texture retrieval using generalized Gaussian density and Kullback-Leibler distance. *IEEE Trans. Image Process.*, 11(2):146–158, 2002.
- [5] E.Paquet, M.Rioux, A.Murching, T.Naveen, and A.Tabatabai. Description of shape information for 2-d and 3-d objects. *Signal Processing: Image Communication*, 16(1-2):103–122, 2000.
- [6] T. A. Funkhouser, P. Min, M. M. Kazhdan, J. Chen, J. A. Halderman, D. P. Dobkin, and D. P. Jacobs. A search engine for 3d models. *ACM Trans. Graph.*, 22(1):83–105, 2003.
- [7] M. Hilaga, Y. Shinagawa, T. Kohmura, and T. L. Kunii. Topology matching for fully automatic similarity estimation of 3d shapes. In *Proceedings of the 28th annual conference on Computer graphics and interactive techniques*, pages 203–212. ACM Press, 2001.
- [8] H. Hoppe and E. Praun. Shape compression using spherical geometry images. In *MINGLE 2003 Workshop. In Advances in Multiresolution for Geometric Modelling*, pages 27–46, 2003.
- [9] N. Iyer, S. Jayanti, K. Lou, Y. Kalyanaraman, and K. Ramani. Three-dimensional shape searching: state-of-the-art review and future trends. *Computer-Aided Design*, 37(5):509–530, 2005.
- [10] C. E. Jacobs, A. Finkelstein, and D. H. Salesin. Fast multiresolution image querying. In *SIGGRAPH '95*, pages 277–286, NY, USA, 1995.
- [11] A. Johnson. *Spin-Images: A Representation for 3-D Surface Matching*. PhD thesis, Robotics Institute, Carnegie Mellon University, Pittsburgh, PA, August 1997.
- [12] M. Kazhdan, T. Funkhouser, and S. Rusinkiewicz. Rotation invariant spherical harmonic representation of 3d shape descriptors. In *SGP '03: Eurographics/ACM SIGGRAPH symposium on Geometry processing*, pages 156–164, Switzerland, 2003. Eurographics Association.
- [13] M. Novotni and R. Klein. 3d zernike descriptors for content based shape retrieval. In *SM '03: Proceedings of the eighth ACM symposium on Solid modeling and applications*, pages 216–225, NY, USA, 2003. ACM Press.
- [14] M. Novotni and R. Klein. Shape retrieval using 3d zernike descriptors. *Computer-Aided Design*, 36(11):1047–1062, 2004.
- [15] R. Osada, T. Funkhouser, B. Chazelle, and D. Dobkin. Matching 3d models with shape distributions. In *Shape Modeling International*, pages 154–166, Genova, Italy, May 2001.
- [16] D. Saupe and D. V. Vranic. 3d model retrieval with spherical harmonics and moments. In B. Radig and S. Florczyk, editors, *DAGM-Symposium*, volume 2191 of *Lecture Notes in Computer Science*, pages 392–397. Springer, 2001.
- [17] P. Schroder and W. Sweldens. Spherical wavelets: efficiently representing functions on the sphere. In *SIGGRAPH '95*, pages 161–172, NY, USA, 1995. ACM Press.
- [18] P. Shilane, P. Min, M. Kazhdan, and T. Funkhouser. The princeton shape benchmark. In *Shape Modeling International 2004, Genova, Italy*, june 2004.
- [19] H. Sundar, D. Silver, N. Gagvani, and S. J. Dickinson. Skeleton based shape matching and retrieval. In *Shape Modeling International*, pages 130–142, 2003.
- [20] J. W. Tangelder and R. C. Veltkamp. A survey of content based 3d shape retrieval. In *Shape Modeling International 2004, Genova, Italy*, pages 145–156, June 2004.
- [21] G. van de Wouwer, P. Scheunders, and D. van Dyck. Statistical texture characterization from discrete wavelet representations. *IEEE trans. on Image Processing*, 8(4):592–598, April 1999.
- [22] D. V. Vranic. An improvement of rotation invariant 3d-shape based on functions on concentric spheres. In *ICIP2003*, pages 757–760, 2003.
- [23] D. V. Vranic. *3D Model Retrieval*. Phd dissertation, Universitat Leipzig, Institut Fur Informatik, 2003.